Adenovirus-mediated overexpression of bone morphogenetic protein-9 promotes methionine choline deficiency-induced non-alcoholic steatohepatitis in non-obese mice

QI LI[1*], BEIBEI LIU[2*], KATJA BREITKOPF-HEINLEIN[3], HONGLEI WENG[3], QIANQIAN JIANG[2], PEILING DONG[1], STEVEN DOOLEY[3], KESHU XU[2**] and HUIGUO DING[1**]

[1]Department of Hepatology and Gastroenterology, Beijing You An Hospital, Capital Medical University, Beijing 100069; [2]Division of Gastroenterology, Union Hospital, Tongji Medical College, Huazhong University of Science and Technology, Wuhan, Hubei 430022, P.R. China; [3]Department of Medicine II, Medical Faculty Mannheim, Heidelberg University, D-68167 Mannheim, Germany

Received December 4, 2018; Accepted May 20, 2019

DOI: 10.3892/mmr.2019.10508

Abstract. Liver inflammation and macrophage infiltration are critical steps in the progression of non-alcoholic fatty liver to the development of non-alcoholic steatohepatitis. Bone morphogenetic protein-9 is a cytokine involved in the regulation of chemokines and lipogenesis. However, the function of bone morphogenetic protein-9 in non-alcoholic steatohepatitis is still unknown. The present study hypothesized that bone morphogenetic protein-9 may contribute to steatohepatitis in mice fed a methionine choline deficiency diet (MCD). C57BL/6 mice overexpressing bone morphogenetic protein-9 and control mice were fed the MCD diet for 4 weeks. Liver tissue and serum samples were obtained for subsequent measurements. Bone morphogenetic protein-9 overexpression exacerbated steatohepatitis in mice on the MCD diet, as indicated by liver histopathology, increased serum alanine aminotransferase activity, aspartate transaminase activity, hepatic inflammatory gene expression and M1 macrophage recruitment. Although bone morphogenetic protein-9 overexpression did not affect the expression of pro-fibrogenic genes, including Collagen I (α)1 or matrix metalloproteinase (MMP) 9, it did upregulate the expression of transforming growth factor-β and plasminogen activator inhibitor 1, and downregulated the expression of MMP2. The above results indicate that bone morphogenetic protein-9 exerts a pro-inflammatory role in MCD diet-induced non-alcoholic steatohepatitis.

Correspondence to: Professor Huiguo Ding, Department of Hepatology and Gastroenterology, Beijing You An Hospital, Capital Medical University, 8 You'anmenwai Street, Beijing 100069, P.R. China
E-mail: dinghuiguo@medmail.com.cn

Professor Keshu Xu, Division of Gastroenterology, Union Hospital, Tongji Medical College, Huazhong University of Science and Technology, 1277 Jiefang Road, Wuhan, Hubei 430022, P.R. China
E-mail: xl2017@hust.edu.cn

*,**Contributed equally

Abbreviations: NASH, non-alcoholic steatohepatitis; BMP-9, bone morphogenetic protein-9; TGF-β, transforming growth factor-β; MCD, methionine choline deficiency; ALT, alanine aminotransferase; AST, aspartate transaminase; CTGF, connective tissue growth factor; PAI-1, plasminogen activator inhibitor 1; MMP-2, matrix metalloproteinase-2; NAFLD, non-alcoholic fatty liver disease; NAFL, non-alcoholic fatty liver; HCC, hepatocellular carcinoma; MCP-1, monocyte chemoattractant protein-1; TNF-α, tumor necrotic factor-α; CCR2, C-C chemokine receptor 2; IL, interleukin; GDF-2, growth differentiation factor-2; Ad-BMP-9-HA(c), adenovirus-mediated over-expression of BMP-9 tagged with HA at the C-terminus; SPF, specific pathogen free; PFU, plaque forming unit; TG, triglyceride; IHC, immunohistochemistry; iNOS, inducible nitric oxide synthase; α-SMA, α-smooth muscle actin; MMP-9, matrix metalloproteinase-9; ALK-1, activin receptor-like kinase-1

Key words: NASH, inflammation, macrophage, BMP-9, fibrosis

Introduction

Non-alcoholic fatty liver disease (NAFLD) includes a broad spectrum of disorders from NAFL to non-alcoholic steatohepatitis (NASH) and steatofibrosis. Histologically, hepatocyte steatosis, hepatocyte ballooning, hepatic inflammation and fibrosis characterize NASH (1). The majority of patients with NAFL present no symptoms; however, ~20% of patients with NAFL progress to NASH, or even cirrhosis, portal hypertension and hepatocellular carcinoma (HCC) (1). Hepatic inflammation is associated with the prognosis of patients with NAFLD. Globally, a total of 40.76% patients with NASH progress to fibrosis and end stage liver disease (2). Until now, only a limited number of established medications for NASH are clinically applicable. Therefore, a better understanding of the underlying mechanisms leading to NAFLD progression is required, which may in turn improve the efficacy of NASH

treatments. During the progression of steatosis to NASH, it has been confirmed that hepatocellular injury and chronic inflammation are the critical mediators (2). This inflammation is associated with recruitment of macrophages to the liver and the expression of pro-inflammatory factors, including the chemokine monocyte chemoattractant protein-1 (MCP-1) and tumor necrotic factor-α (TNF-α) (3). On the basis of lipid toxicity, the generation and secretion of MCP-1 by hepatocytes increases, which in turn interact with C-C chemokine receptor 2 (CCR2) on the surface of macrophages, and mediate the recruitment and activation of liver macrophages. In addition, increased amounts of pro-inflammatory and pro-fibrotic factors are released by liver macrophages. In patients with NASH, the activation of hepatic macrophages and their pro-inflammatory activity are markers of disease progression, which affect fatty degeneration, attract lymphocytes, stimulate angiogenesis and promote liver fibrosis (3). Macrophages differentiate into two cellular subtypes: Pro-inflammatory M1 macrophages and immune-regulatory M2 macrophages. M1 type cells highly express CD86 and CD80, and secrete pro-inflammatory cytokines, including interleukin (IL)-1β and TNF-α, whereas M2 type cells mainly express CD206, CD163 and Arginase 1 (Arg1) and secrete factors such as IL-4 and IL-10 (4). MCP-1 inhibition reduces the infiltration of M1 macrophages and prevents the M2 type transformation to the M1 type, interrupting NASH progression (5,6).

Bone morphogenetic protein-9 (BMP-9), also termed growth differentiation factor-2, belongs to the TGF-β superfamily and was first cloned from a fetal mouse liver cDNA library (7). The precursor of human BMP-9 is comprised of 429 amino acids with a molecular weight of ~47 kDa. Following post-transcriptional modification, the immature precursor is divided into a pro-region and a mature region (13 kDa). However, both dimers of the mature regions and BMP-9 pro-region complexes have the same biological functions after secretion (8). BMP-9 is predominantly produced by the liver and constitutively circulates at relevant physiological levels in the bloodstream of healthy individuals (9). After BMP-9 binding to the type II receptor or the type I receptor on the cell surface, a receptor-complex is formed and the SMAD family member 1 (Smad1) signaling pathway is activated. Phosphorylated Smad1 binds to Smad4 and this complex translocates into the cell nucleus, which regulates the expression of BMP-9 target genes (10). Emerging evidence has indicated that BMP-9 participates in various physiologic processes, including bone formation, glucose homeostasis, iron homeostasis and angiogenesis (11-14). Pathologically, BMP-9 takes part in the occurrence and development of various types of tumors (10) including HCC (15,16). Recently, BMP-9 was found to mediate lipid metabolism and the expression of chemokines (17,18). In endothelial cells, BMP-9 mediated the expression of MCP-1 (17,18).

It has been previously reported that BMP-9 enhances liver fibrogenesis (19). Kim *et al* (20) further demonstrated that MB109, a recombinant BMP-9 derivative, could induce the hepatic expression of fatty acid synthetase in obese mice and reduced the content of lipid droplets, as well as the serum level of alanine aminotransferase (ALT) and total cholesterol. Although BMP-9 has been shown to ameliorate NAFLD in a high-fat diet model (20), there is no data regarding the role of BMP-9 in the methionine- and choline-deficient (MCD)-diet model of NASH. Therefore, the aim of the present study was to clarify the contribution of BMP-9 to liver disease in mice fed a MCD diet. This model has been widely accepted as the classic model to study the underlying mechanisms of NASH. In the present study, it was demonstrated that adenoviral gene transfer of BMP-9 via the tail vein elevated BMP-9 levels in the liver, and promoted the progression of NASH by inducing the secretion of inflammatory factors and M1 macrophage infiltration.

Materials and methods

Adenoviruses. Adenoviruses Ad-BMP-9-HA(c) and Adnull were commercially purchased from SinoGenoMax Co., Ltd.

Animal model. Specific pathogen free C57BL/6 mice (male, 6 weeks, 18-20 g) were used in the present study. Mice were maintained in a standard 12-h light/dark cycle environment with a constant temperature (22±2˚C) and humidity (40-60%) and free access to chow and water. The ingredients comprising the MCD are listed in Table SI. A total of 48 mice were divided into four groups: Control, MCD, MCD+Ad-BMP-9-HA(c) and MCD+Adnull group (n=12/group). Six mice in each group were fed their assigned diet for 2 weeks and an additional 6 mice in each group were fed their assigned diet for 4 weeks. In the control group, mice were fed a chow diet and in the MCD groups, mice were fed the MCD diet. In the MCD+adenovirus groups, mice received $1x10^9$ plaque forming unit (PFU) of adenovirus vectors via the tail vein once a week for 4 weeks. Animals were sacrificed 24 h after the end of their 2 and 4 weeks diet periods, respectively. Mouse cardiac blood samples were taken to measure ALT and aspartate transaminase (AST) levels. Liver tissues were fixed in 4% paraformaldehyde at room temperature for >24 h or frozen for subsequent staining experiments. The remaining liver tissues were frozen at -80˚C and subsequently used for reverse transcription-quantitative (RT-qPCR).

All animal experiments were approved by the Animal Care and Use Committee at Tongji Medical College, Huazhong University of Science and Technology and in full compliance with Hubei Province Laboratory Animal Care Guidelines for the use of animals in research (21).

ALT, AST and liver triglyceride (TG) content measurement. The serum levels of ALT/AST and the liver TG content were determined using commercially available reagents (ALT:C009-2, AST:C0010-2 and TG:A110-1; Nanjing Jiancheng Bioengineering Institute) according to the manufacturer's instructions.

Histology and immunohistochemistry (IHC). Mouse liver tissues were fixed in 4% paraformaldehyde at room temperature for >24 h, and embedded in paraffin. For hematoxylin-eosin (H&E) staining, liver sections (4 μm) were dewaxed, stained with hematoxylin for 5 min and differentiated with 1% hydrochloric acid alcohol for 5-10 sec, then stained with eosin and followed by dehydration. For Sirius red staining, dewaxed liver sections were stained with Sirius red stain for 1 h and Mayer hematoxylin stain for 10 min. For Oil red O staining, frozen

liver sections (8 μm) were fixed in 4% paraformaldehyde for 10 min and washed with deionized water, then stained with Oil Red O working solution (Sigma-Aldrich) for 10 min at room temperature and washed in deionized water, and finally stained with hematoxylin. IHC staining was performed as previously described (15). Briefly, the sections were deparaffinized in xylene, rehydrated in graded ethanol and washed in distilled water. Antigen retrieval was performed with microwave in EDTA buffer (1 mM, pH 8.0) at 100˚C for 15 min. The slides were immersed in 3% H_2O_2 for 30 min at room temperature and then washed with PBS three times. Then, Dako peroxidase blocking reagent (Agilent Technologies, Inc.) was used to block the endogenous peroxidase at room temperature for 15 min. Slides were incubated with primary antibodies including F4/80 (1:200; cat. no. 27044-1-AP; ProteinTech Group, Inc.), inducible nitric oxide synthase (iNOS; 1:200; cat. no. 18985-1-AP; ProteinTech Group, Inc.), CD206 (1:100; cat. no. 18704-1-AP; ProteinTech Group, Inc.) and α-smooth muscle actin (α-SMA; 1:200; cat. no. 14395-1-AP; ProteinTech Group, Inc.) at 4˚C overnight. On the following day, the slides were warmed to the room temperature and washed with PBS three times before being incubated with HRP-conjugated Affinipure Goat Anti-Rabbit IgG(H+L) secondary antibodies (1:200; cat. no. SA00001-2;, ProteinTech Group, Inc.) at room temperature for 1 h. The immune-reactivity were visualized with a Dako REAL EnVision Detection System, Peroxidase/DAB+ kit (cat. no. K5007, Agilent Technologies, Inc.). Then the slides were counterstained with hematoxylin at room temperature for 5 min. All staining images of H&E, Sirius red, Oil red O and IHC were acquired on a routine light microscope.

For semi-quantitative analysis of the iNOS immunostaining, positively stained cells presenting maximal immune-positivity were counted using a light microscope in four fields in each section at x40 magnification and analyzed using ImageJ software version 1.8.0 (National Institute of Health). The numbers of positively stained macrophages were statistically compared in the 4 groups.

For semi-quantitative analysis of F4/80, α-SMA immunostaining and Sirius red staining, the percentage of positively stained areas were counted in four fields under a microscope at x20 magnification and analyzed using ImageJ software version 1.8.0 (National Institute of Health). The percentage area of positive staining was statistically compared in the 4 groups.

The histological scoring of the liver lesions was evaluated with NAFLD activity score (NAS). The NAS scores for steatosis were 0-3, for lobular inflammation were 0-3 and for ballooning were 0-2; therefore the scores ranged from 0 to 8 (22,23).

RNA isolation, cDNA synthesis and RT-qPCR. Total RNA from cells and liver tissue samples was isolated using TRIzol® Reagent (Takara Biotechnology Co., Ltd.) and reverse transcribed into cDNA using a PrimeScript™ RTase kit (Takara Biotechnology Co., Ltd.) according to the manufacturer's protocol (37˚C for 15 min, 85˚C for 5 sec, then cooled to 8˚C). RT-qPCR was conducted using the SYBR Green PCR Master Mix (Takara Biotechnology Co., Ltd.). Primer sequences are listed in Table I. cDNA samples were amplified in duplicate using LightCycler 480 Software version 1.5.0 (Roche Diagnostics GmbH). The RT-qPCR thermocycling conditions were as follows: 95˚C for 10 min, followed by 40 cycles of 95˚C for 15 sec and 60˚C for 1 min. Fluorescence data of the target genes were analyzed using the $2^{-\Delta\Delta Cq}$ method (24) for relative quantification using β-actin as a control.

Protein extraction and western blot assay. Total protein samples were extracted by treating liver tissues with RIPA lysis buffer and protease inhibitor cocktail tablets. Proteins were denatured at 100˚C for 10 min, then were stored at -20˚C or used for western blot assay immediately. Proteins were separated by 10% SDS-PAGE Gel (Beyotime, P0012A) and then transferred to polyvinylidene difluoride (PVDF) membranes (EMD Millipore). The membranes with proteins were blocked with 8% skimmed milk at room temperature for 1 h and incubated with BMP9 primary antibodies (1:2,000, AF-3209, R&D Systems) at 4˚C overnight. Then, the membranes were incubated with secondary antibody of Rabbit anti Goat IgG (H L) labeled with HRP (1:2,000, ANT021s, Antgene Biotechnology Co., Ltd.) for 1 h at room temperature. Then immunoreactive protein bands were visualized with chemiluminescence (ECL) kit (P0018S; Beyotime Institute of Biotechnology).

Statistical analysis. The quantitative data were presented as the mean ± standard deviation and presented graphically as the mean ± standard error of the mean. Comparisons between two groups were performed with Student's t-test. Comparisons between multiple groups were performed using one-way analysis of variance and Tukey's multiple comparisons test. $P<0.05$ was considered to indicate a statistically significant comparison.

Results

BMP-9 mRNA expression is significantly induced in the liver tissues of NASH model mice. NASH is histologically diagnosed with hepatocyte steatosis, hepatocyte ballooning and hepatic inflammation (22). In the present study, an MCD-induced NASH model was successfully established, being characterized with hepatocyte steatosis, hepatocyte ballooning and hepatic inflammation in mouse livers. Through RT-qPCR analysis, BMP-9 mRNA levels were measured in the livers of NASH mice (induced by MCD diet). BMP-9 was revealed to be significantly upregulated in MCD-induced NASH mice following 4 weeks when compared with the control mice ($P<0.05$; Fig. 1). This upregulation of BMP-9 expression in the NASH model indicated that BMP-9 may serve a role in the progression of NASH.

Adenovirus mediated-BMP-9 overexpression in the liver aggravates MCD-induced NASH in mice. BMP-9 tagged with HA at the C-terminus [Ad-BMP-9-HA(c)] with or without (Adnull) adenovirus under the transcriptional control of the cytomegalovirus promoter was used for infection experiments in mice. At 2 weeks, BMP-9 mRNA expression was increased in BMP-9 overexpressing mice, and the mRNA and protein expression levels of BMP-9 were confirmed in the liver tissues of C57BL/6 mice after tail vein injection of $1x10^9$ PFU Ad-BMP-9-HA(c) once a week for 4 weeks (Figs. 2A, and 3A and B).

H&E and Oil red-stained slides were examined by a pathologist. Mice fed the MCD diet developed panacinar

Table I. Primer sequences for reverse transcription-quantitative PCR.

Primer	Forward (5'-3')	Reverse (5'-3')
β-actin	GGCTGTATTCCCCTCCATCG	CCAGTTGGTAACAATGCCATGT
BMP-9	CAGAACTGGGAACAAGCATCC	GCCGCTGAGGTTTAGGCTG
CCR2	ATCCACGGCATACTATCAACATC	CAAGGCTCACCATCATCGTAG
Collagen Ia1	GCTCCTCTTAGGGGCCACT	CCACGTCTCACCATTGGGG
TGF-β1	CTCCCGTGGCTTCTAGTGC	GCCTTAGTTTGGACAGGATCTG
α-SMA	GTCCCAGACATCAGGGAGTAA	TCGGATACTTCAGCGTCAGGA
MMP-2	CAAGTTCCCCGGCGATGTC	TTCTGGTCAAGGTCACCTGTC
MMP-9	CTGGACAGCCAGACACTAAAG	CTCGCGGCAAGTCTTCAGAG
CTGF	GGGCCTCTTCTGCGATTTC	ATCCAGGCAAGTGCATTGGTA
MCP-1	ATCCACGGCATACTATCAACATC	CAAGGCTCACCATCATCGTAG
TNF-α	CCCTCACACTCAGATCATCTTCT	GCTACGACGTGGGCTACAG
IL-10	GCTCTTACTGACTGGCATGAG	CGCAGCTCTAGGAGCATGTG
PAI-1	TTCAGCCCTTGCTTGCCTC	ACACTTTTACTCCGAAGTCGGT
F4/80	TGACTCACCTTGTGGTCCTAA	CTTCCCAGAATCCAGTCTTTCC
iNOS	GTTCTCAGCCCAACAATACAAGA	GTGGACGGGTCGATGTCAC
IL-1β	GCAACTGTTCCTGAACTCAACT	ATCTTTTGGGGTCCGTCAACT
IL-6	TAGTCCTTCCTACCCCAATTTCC	TTGGTCCTTAGCCACTCCTTC
IL-12	TGGTTTGCCATCGTTTTGCTG	ACAGGTGAGGTTCACTGTTTCT
IL-17	TCAGCGTGTCCAAACACTGAG	CGCCAAGGGAGTTAAAGACTT

BMP-9, bone morphogenetic protein-9; CCR2, C-C chemokine receptor-2; TGF-β1, transforming growth factor-β1; α-SMA, α-smooth muscle actin; MMP-2, matrix metalloproteinase-2; MMP-9, matrix metalloproteinase-9; CTGF, connective tissue growth factor; MCP-1, monocyte chemoattractant protein-1; TNF-α, tumor necrosis factor-α; IL-10, interleukin-10; PAI-1, plasminogen activator inhibitor 1; iNOS, inducible nitric oxide synthase; IL, interleukin.

macrovesicular hepatic steatosis. Compared with the control, in the MCD and MCD+Adnull groups at 2 weeks, the mouse livers with BMP-9 overexpression exhibited enhanced hepatocyte ballooning, focal inflammatory cell infiltration and bullous steatosis (Fig. 2B-D), which were further intensified at 4 weeks (Fig. 3C-E).

At 2 weeks, serum AST levels were significantly increased in mice when comparing the MCD diet to the control (167.91±21.35 vs. 89.76±37.11 U/l; P<0.05) and were even higher in BMP-9 overexpressing mice fed the MCD diet (MCD diet+AdBMP-9 vs. MCD diet+Adnull (253.69±34.27 vs. 146.52±21.89 U/l; P<0.01; Fig. 2E). ALT was not increased with the MCD diet (control vs. MCD diet: 82.58±12.98 vs. 138.06±21.29 U/l; P>0.05); however, a significant increase in the MCD mice with BMP-9 overexpression was observed (MCD diet+Adnull vs. MCD diet+AdBMP-9: 113.43±16.08 vs. 465.74.4±54.13 U/l; P<0.001; Fig. 2F). Liver TG levels were reported to be similar to those of AST (control vs. MCD diet: 6.05±2.12 vs. 9.47±1.94 mg/g liver; P>0.05; MCD diet+Adnull vs. MCD diet+AdBMP-9: 11.76±2.52 vs. 22.09±6.01 mg/g liver; P<0.05; Fig. 2G).

At 4 weeks, serum AST levels were significantly increased in mice on the MCD diet (control vs. MCD diet; 14.18±2.52 vs. 51.62±11.30 U/l; P<0.05) and were even higher in BMP-9 overexpressing mice fed the MCD diet (MCD diet+Adnull vs. MCD diet+AdBMP-9; 54.55±13.88 vs. 254.3±62.46 U/l; P<0.01; Fig. 3F). The same was observed for ALT (control vs. MCD diet; 44.27±3.66 vs. 77.3±5.27 U/l; P<0.05; MCD diet+Adnull vs. MCD diet+AdBMP-9: 125.4±45.56 vs. 359.8±57.55 U/l; P<0.01; Fig. 3G). An increase in liver TG was also observed in MCD mice (control vs. MCD diet: 8.78±0.83 vs. 12.71±0.83 mg/g liver; P<0.05), whereas no significant differences were observed in BMP-9 overexpression (MCD diet+Adnull vs. MCD diet+AdBMP-9: 10.18±2.42 vs. 10.57±1.45 mg/g liver; P>0.05; Fig. 3H).

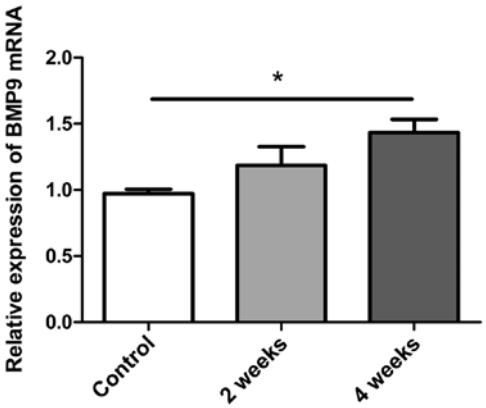

Figure 1. Quantitative analysis of BMP-9 expression in the MCD-induced NASH mouse model. Bar graphs presenting the results of the quantitative analysis of the mRNA expression of BMP-9 over time in liver tissues obtained from MCD-induced NASH model mice. *P<0.01, as indicated. Data are presented as the mean ± standard error of the mean. BMP-9, bone morphogenetic protein-9; MCD, methionine- and choline-deficient diet; NASH, non-alcoholic steatohepatitis.

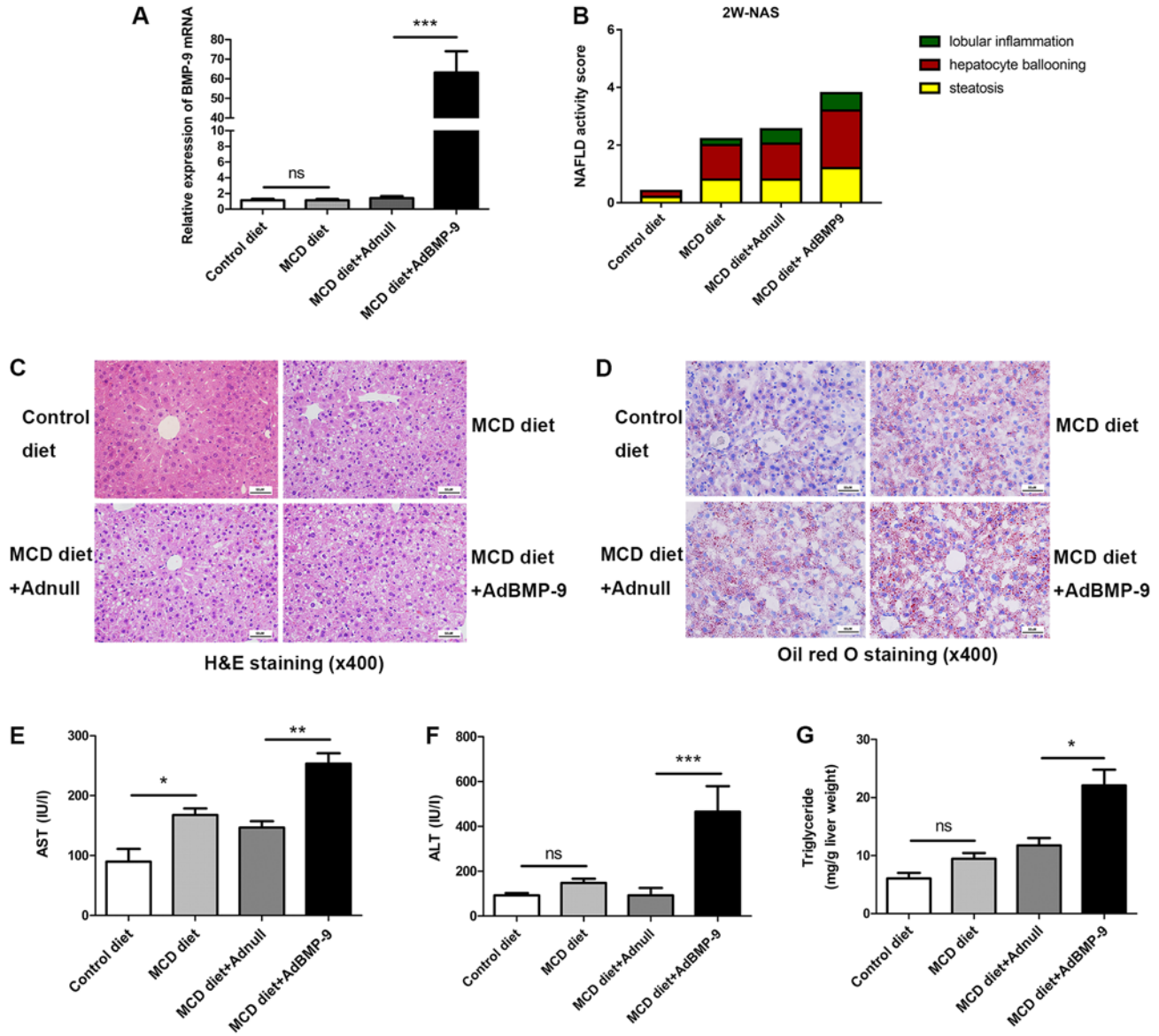

Figure 2. Effect of BMP-9 overexpression on liver histology, serum ALT, serum AST and liver triglyceride levels in mice fed the MCD diet for 2 weeks. BMP-9 overexpressing and wild type mice, both with a C57BL/6 genetic background, were fed either the control diet or the MCD diet for 2 weeks. (A) Bar graphs presenting the results of the quantitative analysis of the mRNA expression of BMP-9 in the liver tissues of the 4 groups. (B) The NAS for the 4 different groups. (C) Representative photomicrographs of H&E-stained and (D) Oil Red-stained liver tissues for the 4 groups (magnification, x400). (E) Bar graphs presenting the results of the quantitative analysis of serum AST, (F) serum ALT and (G) liver triglyceride levels in the 4 groups. *P<0.05, **P<0.01 and ***P<0.001, as indicated. Data are expressed as the mean ± standard error of the mean (n=6 mice in each group). NAFLD, non-alcoholic fatty liver disease; NAS, NAFLD activity score; BMP-9, bone morphogenetic protein-9; MCD, methionine- and choline-deficient diet; ALT, alanine aminotransferase; AST, aspartate transaminase; ns, not significant; H&E, hematoxylin and eosin.

These results implied that BMP-9 exacerbates hepatocyte damage and enhances MCD-induced NASH in mice.

BMP-9 overexpression induces inflammatory gene expression in MCD-induced NASH mice. Since inflammation is a critical factor in the progression of fatty liver to NASH (25). The present study investigated BMP-9 overexpression-induced enhancement of focal inflammatory cell infiltration in MCD mice. In addition, the expression of a number of inflammatory genes was examined. At both 2 and 4 weeks, when compared with mice administered the MCD diet, the mRNA expression levels of MCP-1 were increased in the livers of MCD mice (Fig. 4A). BMP-9 overexpression in the liver further enhanced the increase in MCP-1 mRNA expression at 2 and 4 weeks (P<0.05; Figs. 4A and 5A). For F4/80, IL-1β and IL-12, BMP-9 overexpression significantly enhanced mRNA expression at both time points compared with the MCD diet+Adnull group (Figs. 4D, F and I, and 5D, F and I). For the mRNA expression levels of CCR2 and IL-17, no significant differences were observed for BMP-9 overexpression at both time points (Figs. 4C and J, and Fig. 5C and J). However, there was a tendency for BMP-9 to reduce IL-10 expression at both time points when compared with MCD diet+Adnull (Figs. 4H and 5H). Despite the fact that TNF-α mRNA expression was enhanced at 2 weeks by BMP-9 overexpression, no significant difference was identified at 4 weeks (Figs. 4B and 5B). By contrast, unlike TNF-α mRNA expression, iNOS mRNA was significantly increased at 4 weeks with BMP-9 overexpression but not at 2 weeks (Figs. 4E and 5E).

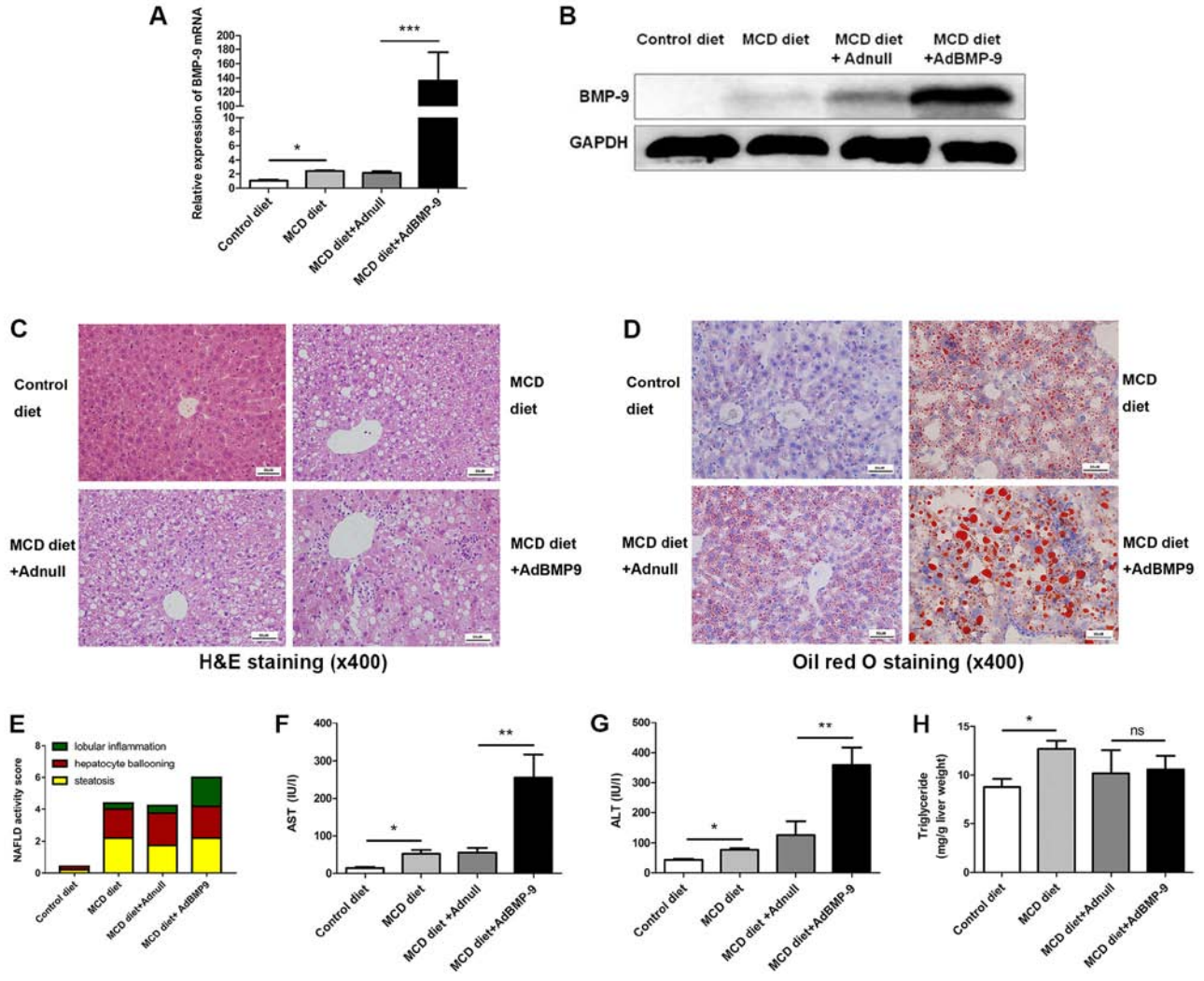

Figure 3. Effect of BMP-9 overexpression on liver histology, serum ALT, serum AST and liver triglyceride levels in mice fed the MCD diet for 4 weeks. BMP-9 overexpressing and wild type mice, both with a C57BL/6 genetic background, were fed either the control diet or the MCD diet for 4 weeks. (A) Bar graphs presenting the results of the quantitative analysis of the mRNA expression of BMP-9 in the liver tissues of the 4 groups. (B) Western blotting of the protein expression of BMP-9 in the liver tissues of the 4 groups. (C) Representative photomicrographs of H&E-stained and (D) Oil Red-stained liver tissues for the 4 groups (magnification, x400). (E) The NAS for the 4 different groups. (F) Bar graphs presenting the results of the quantitative analysis of serum AST, (G) serum ALT and (H) liver triglyceride levels in the 4 groups. *P<0.05, **P<0.01 and ***P<0.001, as indicated. Data are expressed as the mean ± standard error of the mean (n=6 mice in each group). NAFLD, non-alcoholic fatty liver disease; NAS, NAFLD activity score; BMP-9, bone morphogenetic protein-9; MCD, methionine- and choline-deficient diet; ALT, alanine aminotransferase; AST, aspartate transaminase; ns, not significant; H&E, hematoxylin and eosin.

BMP-9 overexpression mediates macrophage accumulation and polarization in MCD-induced NASH model mice. Scattered sinusoidal macrophage staining (using antibodies against F4/80) was present in the livers of MCD mice (Fig. 6). Hepatic macrophage accumulation increased in mice that were administered the MCD diet, which was further increased with BMP-9 overexpression (Fig. 6A and B). The number of iNOS positive macrophages, marked as M1 macrophages that promote inflammation, was significantly higher in the MCD+Ad-BMP-9-HA(c) group when compared with the other 3 groups (Fig. 6D and E); whereas, no staining or significant differences were observed for CD206 positive macrophages, marked as M2 macrophages that secrete anti-inflammatory factors to regulate immunity, in the 4 groups (Fig. 6C). This demonstrates that in the MCD-induced NASH model, macrophages in the liver were more polarized to inflammation, whereby BMP-9 enhanced this pro-inflammatory environment in the development of NASH.

BMP-9 overexpression partly mediates pro-fibrotic gene expression in MCD-induced NASH model mice. We previously reported that BMP-9 is pro-fibrogenic upon liver damage (19). The present study also determined whether BMP-9 promotes liver fibrosis in the NASH model. Since activation of hepatic stellate cells (HSCs) is a key event during liver fibrosis, the expression of α-SMA, a typical marker of activated HSCs was determined by IHC. No significant difference were identified in Sirius red staining intensities among the 4 groups (Fig. 7A and B). Although α-SMA staining increased in the MCD groups, there was no marked difference between the MCD diet+AdBMP-9 and MCD diet+Adnull groups (Fig. 7C and D).

Regarding pro-fibrogenic gene expression, no significant difference for Collagen I was detected in the 4 groups (Fig. 7E and J). However, CTGF, PAI-1 and TGF-β1 were significantly upregulated by the MCD diet. For PAI-1 and TGF-β1, this was further intensified by BMP-9 overexpression; however, BMP-9 overexpression did not significantly

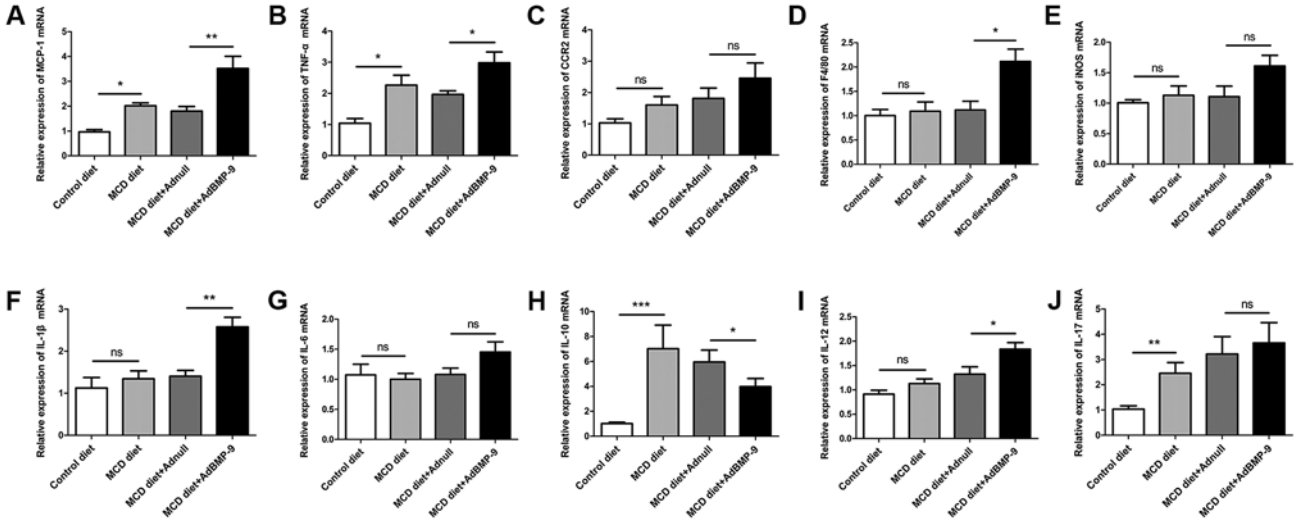

Figure 4. Effect of BMP-9 overexpression on hepatic pro-inflammatory gene mRNA levels in mice fed the MCD diet for 2 weeks. BMP-9 overexpressing and wild type mice were fed either the control diet or the MCD diet for 2 weeks. (A) Bar graphs presenting the results of the quantitative analysis of the mRNA expression of MCP-1, (B) TNF-α, (C) CCR2, (D) F4/80, (E) iNOS, (F) IL-1β, (G) IL-6, (H) IL-10, (I) IL-12 and (J) IL-17 in the liver tissues obtained from the 4 groups. *P<0.05, **P<0.01 and ***P<0.001, as indicated. Data are expressed as the mean ± standard error of the mean (n=6 mice in each group). BMP-9, bone morphogenetic protein-9; MCD, methionine- and choline- deficient diet; ns, not significant; MCP-1, monocyte chemoattractant protein-1; TNF-α, tumor necrotic factor-α; CCR2, C-C chemokine receptor 2; IL, interleukin; iNOS, inducible nitric oxide synthase.

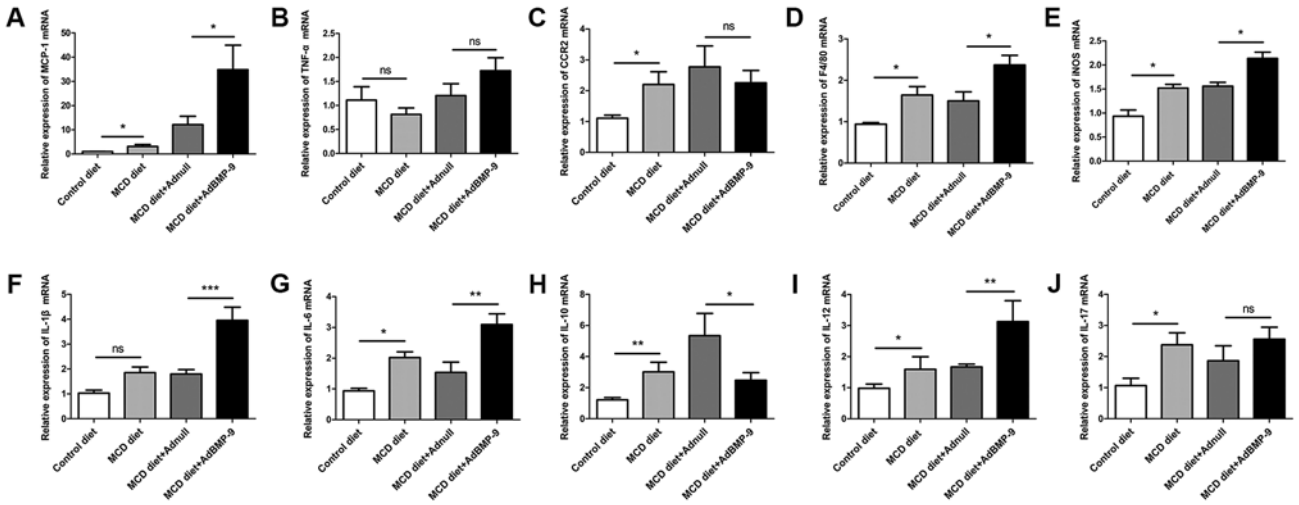

Figure 5. Effect of BMP-9 overexpression on hepatic pro-inflammatory gene mRNA levels in mice fed the MCD diet for 4 weeks. BMP-9 overexpressing and wild-type mice were fed either the control diet or the MCD diet for 4 weeks. (A) Bar graphs presenting the results of the quantitative analysis of the mRNA expression of MCP-1, (B) TNF-α, (C) CCR2, (D) F4/80, (E) iNOS, (F) IL-1β, (G) IL-6, (H) IL-10, (I) IL-12 and (J) IL-17 in the liver tissues obtained from the 4 groups. *P<0.05, **P<0.01 and ***P<0.001, as indicated. Data are expressed as the mean ± standard error of the mean (n=6 mice in each group). BMP-9, bone morphogenetic protein-9; MCD, methionine- and choline-deficient diet; ns, not significant; MCP-1, monocyte chemoattractant protein-1; TNF-α, tumor necrotic factor-α; CCR2, C-C chemokine receptor 2; IL, interleukin; iNOS, inducible nitric oxide synthase.

decrease CTGF expression (Fig. 7F-H). The expression of MMP-2, an extracellular matrix remodeling enzyme, was enhanced by MCD; however, its expression was reduced by BMP-9 overexpression (Fig. 7I). For MMP-9, no differences were observed in the 4 groups. These results indicated that BMP-9 exerts minor pro-fibrotic effects in experimental settings.

Discussion

In the present study, it was indicated that the tail vein injection of Ad-BMP-9-HA(c) induced the overexpression of BMP-9 in the liver, increased the hepatic expression of BMP-9 and exacerbated MCD diet-induced NASH development in mice. To the best of our knowledge, a limited number of studies on the effects of BMP-9 on NASH have been conducted. The results of the present study demonstrated that BMP-9 overexpression enhances MCP-1 expression and promotes macrophage recruitment and polarization in the liver, leading to more acute hepatocyte ballooning, hepatic inflammation and liver fibrosis. BMP-9 overexpression in MCD-fed mice increased the serum levels of ALT and AST; however, the TG contents in the liver at 4 weeks was unchanged. To the best of our knowledge, there is a limited number of reports on the

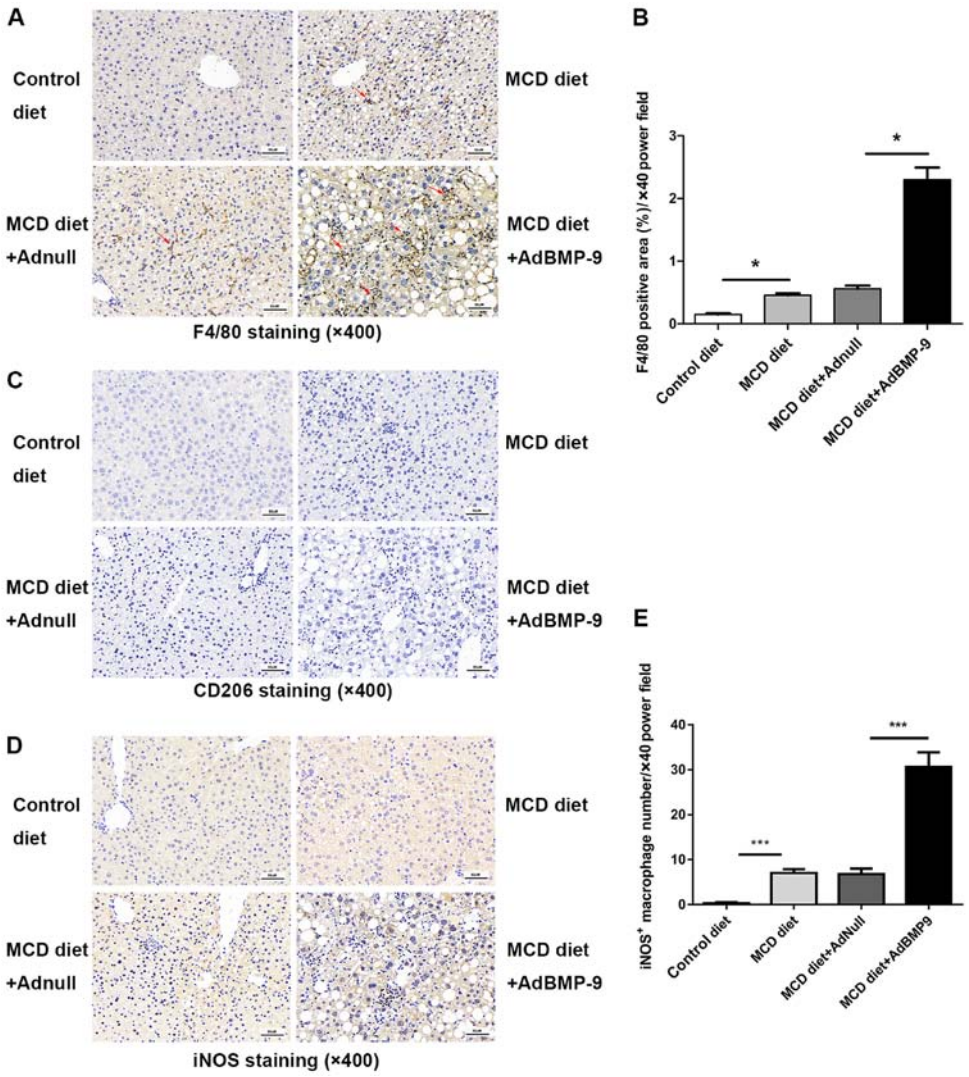

Figure 6. Effect of BMP-9 overexpression on hepatic macrophage accumulation. BMP-9 overexpressing and wild-type mice were fed either the control diet or the MCD diet for 4 weeks. (A) Representative photomicrographs of F4/80-positive staining (indicating macrophages) in the livers of each group (magnification, x400). (B) The extent of F4/80-positive macrophage accumulation was assessed by a pathologist who was blinded to the groups and each tissue was assigned a score (1-10); bar graphs present the results of the quantitative analysis of F4/80-positive macrophage accumulation in the 4 groups. (C) Representative photomicrographs of CD206-positive staining (indicating M2-macrophage) in the livers of each group (magnification, x400). (D) Representative photomicrographs of iNOS-positive staining (indicating M1-macrophages) in the livers of each group (magnification, x400). (E) The extent of iNOS-positive macrophage accumulation was assessed by a pathologist who was blinded to the groups and each tissue was assigned a score (1-10); bar graphs present the results of the quantitative analysis of iNOS-positive macrophage accumulation in the 4 groups. *P<0.05 and ***P<0.001, as indicated. Data are expressed as the mean ± standard error of the mean (n=6 mice in each group). The red arrows indicate the positively stained cells. BMP-9, bone morphogenetic protein-9; MCD, methionine- and choline-deficient diet; iNOS, inducible nitric oxide synthase.

potential role of BMP-9 in fatty liver disease. Kim *et al* (20) reported that periodical injection of MB109, a recombinant derivative of human BMP-9, into high fat diet-induced obese mice not only suppressed weight gain in mice, but also reduced the amount of lipid droplets in the liver, the serum levels of ALT and total cholesterol. In the present MCD models, mice lost weight in a time-dependent manner (Fig. S1), but BMP-9 overexpression in MCD-fed mice increased the serum levels of ALT and AST. These different results from the two studies may be due to the use of different animal models. The high fat diet-induced obese model is normally used to evaluate the insulin resistance of fatty liver; however, the MCD diet has been widely accepted to evaluate mechanisms underlying NASH in rodents. Furthermore, MB109 may not possess all of the natural functions of the full BMP-9 protein.

In our previous study, it was indicated that BMP-9 stimulation of cultured primary hepatocytes inhibited proliferation, epithelial to mesenchymal transition and preserved the expression of important metabolic enzymes, including cytochrome P450 oxidases (19). Application of BMP-9 after partial hepatectomy also significantly enhanced liver damage and disturbed the proliferative response (19). In the NASH model utilized in the present study (MCD model), it was further demonstrated that BMP-9 overexpression enhanced ALT and AST serum levels and hepatocyte ballooning, indicating that BMP-9 promoted liver damage.

Aside from enhancing liver damage, we also previously demonstrated that BMP-9 plays a pro-fibrogenic role *in vivo*. Chronic carbon tetrachloride challenge in BMP-9-deficient mice or in mice adenovirally overexpressing the selective

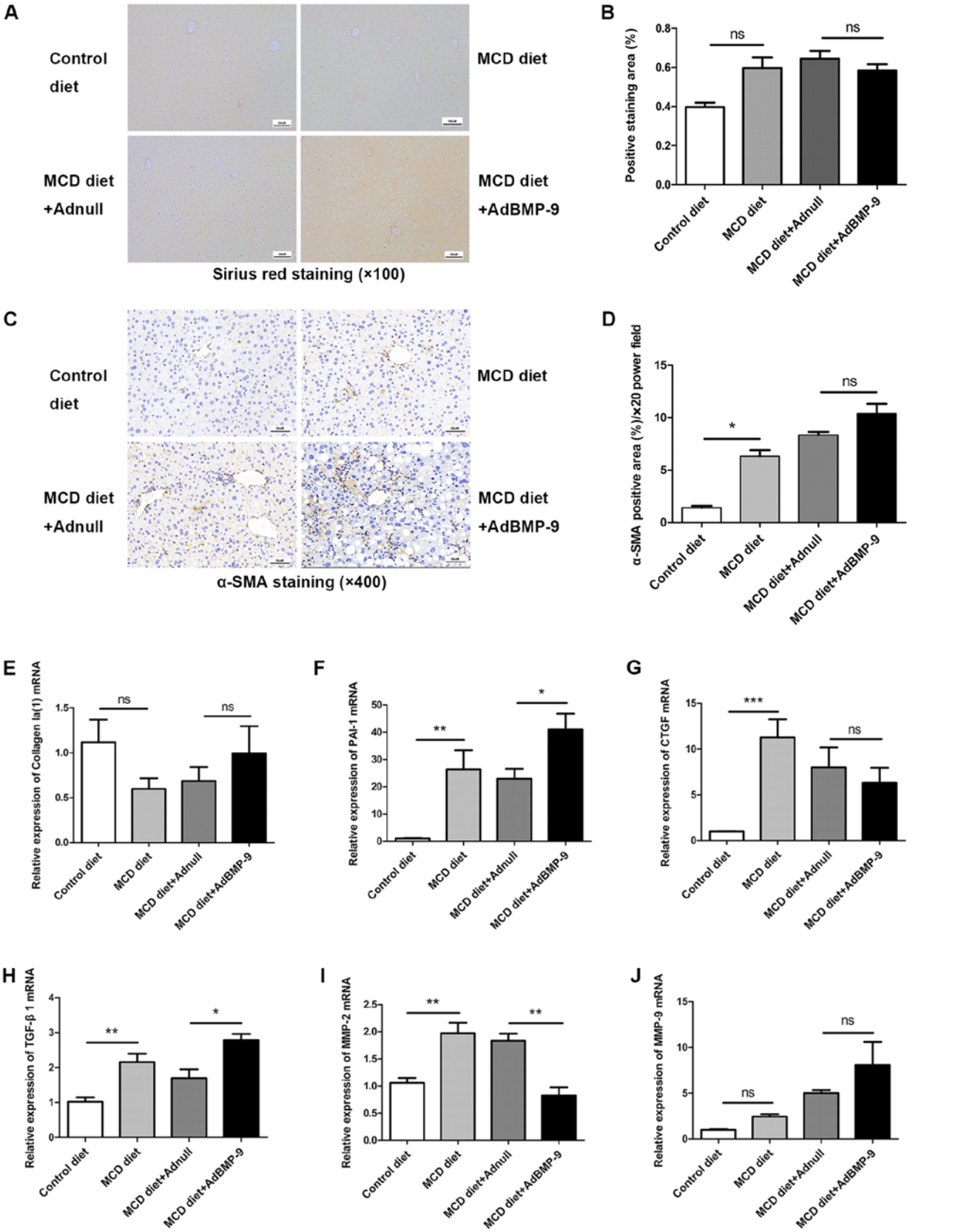

Figure 7. Effect of BMP-9 overexpression on liver fibrosis in mice fed the MCD diet. BMP-9 overexpressing and wild-type mice were fed either the control diet or the MCD diet for 4 weeks. (A) Representative photomicrographs of Sirius red staining in the livers of each group (magnification, x100). (B) The extent of Sirius red staining was assessed via semi-quantification; bar graphs present the results of the semi-quantitative analysis of Sirius red staining in the 4 groups. (C) Representative photomicrographs of α-SMA immunostaining in the livers of each group (magnification, x400). (D) The extent of α-SMA immunostaining was assessed via semi-quantification; bar graphs present the results of the semi-quantitative analysis of α-SMA staining in the 4 groups. (E) Bar graphs presenting the results of the quantitative analysis of the mRNA expression of Collagen Ia(1), (F) PAI-1, (G) CTGF, (H) TGF-β1, (I) MMP-2 and (J) MMP-9 in the liver tissues of the 4 groups. *P<0.05, **P<0.01 and ***P<0.001, as indicated. Data are expressed as the mean ± standard error of the mean (n=6 mice in each group). BMP-9, bone morphogenetic protein-9; MCD, methionine- and choline-deficient diet; TGF-β, transforming growth factor-β; CTGF, connective tissue growth factor; PAI-1, plasminogen activator inhibitor 1; MMP, matrix metalloproteinase; α-SMA, α-smooth muscle actin; ns, not significant.

BMP-9 antagonist activin receptor-like kinase-1-Fc resulted in reduced collagen deposition and subsequent fibrosis (19). Li *et al* (26) further confirmed that in patients, higher BMP-9 levels were associated with advanced stages of liver fibrosis, and in mouse models recombinant BMP-9 overexpression accelerated liver fibrosis and adenoviruses-mediated BMP-9 knockdown attenuated liver fibrogenesis. In the MCD NASH model, the present study indicated that although BMP-9 overexpression induced TGF-β1 and PAI-1 expression, it failed to significantly enhance collagen deposition, and stellate cell activation marked by α-SMA positivity in the liver was not promoted by BMP-9. However, in addition to upregulating TGF-β1 and PAI-1, BMP-9 also downregulated the expression of MMP-2, both representing pro-fibrotic features. Flores-Costa *et al* (27) revealed that in mice with NASH, MMP-2 expression was increased, which is consistent with the results of the present study. The present study demonstrated that BMP-9 significantly inhibited MMP-2 expression in the liver of MCD-induced NASH model mice. Since MMP-2 is an antifibrotic enzyme, its inhibition can lead to the progression of liver fibrosis (28). Therefore, the present study hypothesized that BMP-9 overexpression may promote NASH fibrosis though MMP-2 downregulation, a subject that requires further examination. However, significantly enhanced collagen deposition at 4 weeks was simply too short. Therefore, whether BMP-9 could promote liver fibrosis in NASH requires further investigation.

MCP-1 has been reported to contribute to the pathogenesis of NASH through multiple mechanisms, including enhancement of hepatic lipid accumulation, insulin resistance in mice with a high fat-induced diet, inflammatory responses and liver fibrosis (29). MCP-1 mediates leukocyte recruitment to the liver via interactions with the CCR2 receptor on inflammatory cells including macrophages (30). BMP-9 has been reported to play a role in inflammation by inducing the expression of E-selectin, which is associated with the initial capture of leukocytes and the inflammatory cytokines IL-8 and IL-6 (31). Appleby *et al* (32) reported that BMP-9 alone did not induce neutrophil recruitment to the endothelium; however, it could enhance lipopolysaccharide-induced leukocyte recruitment to the vascular endothelium. Young *et al* (33) reported that in primary human endothelial cells BMP-9 treatment regulated chemokine secretion, adhesion and inflammation pathways. These responses included the upregulation of the chemokine CXCL12/SDF1 and the downregulation of its receptor CXCR4 (33). It remains unclear whether BMP-9 mediates CCR2/MCP-1 interactions. In the present study, it was revealed that BMP-9 could enhance MCP-1 expression in the MCD-induced NASH model livers, whereas it had no effect on CCR2 expression. Future studies will aim to clarify whether BMP-9 is indeed a mediator of CCR2/MCP-1 interactions in NASH progression.

To the best of our knowledge, there is a limited number of studies regarding the association between macrophage polarization and the BMP family. Rocher and Singla (34) reported that BMP-7 treatment could polarize monocytes into M2 macrophages and increase the expression of anti-inflammatory cytokines via the activations of the PI3K-Akt-mTOR signalling pathway. Martínez *et al* (35) observed that BMP-4 was associated with and promoted M2 macrophages, which promote tumor progression in bladder cancer. To the best of our knowledge, there are currently no reports regarding whether BMP-9 was directly associated with macrophage polarization. In the NASH mouse model, the present study demonstrated that BMP-9 overexpression could induce the expression of MCP-1, a chemokine that is characteristic of M1 polarization (36). By contrast, the number of iNOS positive macrophages was significantly increased by BMP-9 overexpression, which further indicates that BMP-9 may play a role in the activation of M1-macrophages, fatty tissue inflammation and NASH. In addition, these results also imply that BMP-9 may play a role in inflammation and macrophage polarization.

In conclusion, the results of the present study revealed that BMP-9 overexpression affected liver steatosis, macrophage recruitment and polarization in MCD diet-mice. In addition, BMP-9 influenced the gene expression of some pro-fibrogenic genes in this model. These results highlight an important distinction in the mechanism underlying inflammation in the MCD diet model of NASH compared with other models. The MCD diet therefore represents a promising model to further investigate the pro-inflammatory effects of BMP-9 in the future.

Acknowledgements

Not applicable.

Funding

The present study was supported by funding from Research Development Fund of Capital Medical University (grant no. PYZ2017085), Scientific Research Project of You'an Hospital, CCMU, 2018 (grant no. YNKTTS20180129), National Natural Science Foundation (grant no. 81672725), Beijing Natural Science Foundation Program and Scientific Research Key Program of Beijing Municipal Commission of Education (grant no. KZ201810025037), WBE Liver Fibrosis Foundation, (grant no. CFHPC20131023), National Natural Science Foundation of China (grant no. 81370525), the BMBF program LiSyM (grant no. PTJ-FKZ: 031L0043) and the Deutsche Forschungsgemeinschaft (German Research Foundation; grant nos. 393225014 and 394046768-SFB1366).

Availability of data and materials

The datasets used and/or analyzed during the current study are available from the corresponding author on reasonable request.

Authors' contributions

QL, SD and HD conceived and designed the study. BL, QJ and PD performed the experiments and collected the data. QL, KBH, HW, HD and KX analyzed and interpreted the data. QL, HW and SD were major contributors in drafting and revising the manuscript. All authors read and approved the final manuscript.

Ethics approval and consent to participate

All animal experiments were in full compliance with the guidelines for animal care and were approved by the Animal Care Committee of Tongji Medical College, Huazhong University of Science and Technology.

Patient consent for publication

Not applicable.

Competing interests

The authors declare that they have no competing interests.

References

1. Pappachan JM, Babu S, Krishnan B and Ravindran NC: Non-alcoholic fatty liver disease: A clinical update. J Clin Transl Hepatol 5: 384-393, 2017.
2. Younossi ZM, Koenig AB, Abdelatif D, Fazel Y, Henry L and Wymer M: Global epidemiology of nonalcoholic fatty liver disease-Meta-analytic assessment of prevalence, incidence, and outcomes. Hepatology 64: 73-84, 2016.
3. Tacke F: Targeting hepatic macrophages to treat liver diseases. J Hepatol 66: 1300-1312, 2017.
4. Park JK, Shao M, Kim MY, Baik SK, Cho MY, Utsumi T, Satoh A, Ouyang X, Chung C and Iwakiri Y: An endoplasmic reticulum protein, Nogo-B, facilitates alcoholic liver disease through regulation of kupffer cell polarization. Hepatology 65: 1720-1734, 2017.
5. Baeck C, Wehr A, Karlmark KR, Heymann F, Vucur M, Gassler N, Huss S, Klussmann S, Eulberg D, Luedde T, *et al*: Pharmacological inhibition of the chemokine CCL2 (MCP-1) diminishes liver macrophage infiltration and steatohepatitis in chronic hepatic injury. Gut 61: 416-426, 2012.
6. Liaskou E, Zimmermann HW, Li KK, Oo YH, Suresh S, Stamataki Z, Qureshi O, Lalor PF, Shaw J, Syn WK, *et al*: Monocyte subsets in human liver disease show distinct phenotypic and functional characteristics. Hepatology 57: 385-398, 2013.
7. Song JJ, Celeste AJ, Kong FM, Jirtle RL, Rosen V and Thies RS: Bone morphogenetic protein-9 binds to liver cells and stimulates proliferation. Endocrinology 136: 4293-4297, 1995.
8. Brown MA, Zhao Q, Baker KA, Naik C, Chen C, Pukac L, Singh M, Tsareva T, Parice Y, Mahoney A, *et al*: Crystal structure of BMP-9 and functional interactions with pro-region and receptors. J Biol Chem 280: 25111-25118, 2005.
9. David L, Mallet C, Keramidas M, Lamandé N, Gasc JM, Dupuis-Girod S, Plauchu H, Feige JJ and Bailly S: Bone morphogenetic protein-9 is a circulating vascular quiescence factor. Circ Res 102: 914-922, 2008.
10. Herrera B, Dooley S and Breitkopf-Heinlein K: Potential roles of bone morphogenetic protein (BMP)-9 in human liver diseases. Int J Mol Sci 15: 5199-5220, 2014.
11. Bessa PC, Cerqueira MT, Rada T, Gomes ME, Neves NM, Nobre A, Reis RL and Casal M: Expression, purification and osteogenic bioactivity of recombinant human BMP-4, -9, -10, -11 and -14. Protein Expr Purif 63: 89-94, 2009.
12. Chen C, Grzegorzewski KJ, Barash S, Zhao Q, Schneider H, Wang Q, Singh M, Pukac L, Bell AC, Duan R, *et al*: An integrated functional genomics screening program reveals a role for BMP-9 in glucose homeostasis. Nat Biotechnol 21: 294-301, 2003.
13. Suzuki Y, Ohga N, Morishita Y, Hida K, Miyazono K and Watabe T: BMP-9 induces proliferation of multiple types of endothelial cells in vitro and in vivo. J Cell Sci 123: 1684-1692, 2010.
14. Truksa J, Peng H, Lee P and Beutler E: Bone morphogenetic proteins 2, 4, and 9 stimulate murine hepcidin 1 expression independently of Hfe, transferrin receptor 2 (Tfr2), and IL-6. Proc Natl Acad Sci U S A 103: 10289-10293, 2006.
15. Li Q, Gu X, Weng H, Ghafoory S, Liu Y, Feng T, Dzieran J, Li L, Ilkavets I, Kruithof-de Julio M, *et al*: Bone morphogenetic protein-9 induces epithelial to mesenchymal transition in hepatocellular carcinoma cells. Cancer Sci 104: 398-408, 2013.
16. Herrera B, Garcia-Alvaro M, Cruz S, Walsh P, Fernández M, Roncero C, Fabregat I, Sánchez A and Inman GJ: BMP9 is a proliferative and survival factor for human hepatocellular carcinoma cells. PLoS One 8: e69535, 2013.
17. Kuo MM, Kim S, Tseng CY, Jeon YH, Choe S and Lee DK: BMP-9 as a potent brown adipogenic inducer with anti-obesity capacity. Biomaterials 35: 3172-3179, 2014.
18. Young K, Tweedie E, Conley B, Ames J, FitzSimons M, Brooks P, Liaw L and Vary CP: BMP9 crosstalk with the hippo pathway regulates endothelial cell matricellular and chemokine responses. PloS One 10: e0122892, 2015.
19. Breitkopf-Heinlein K, Meyer C, Konig C, Gaitantzi H, Addante A, Thomas M, Wiercinska E, Cai C, Li Q, Wan F, *et al*: BMP-9 interferes with liver regeneration and promotes liver fibrosis. Gut 66: 939-954, 2017.
20. Kim S, Choe S and Lee DK: BMP-9 enhances fibroblast growth factor 21 expression and suppresses obesity. Biochim Biophys Acta 1862: 1237-1246, 2016.
21. Chen LL, Yang WH, Zheng J, Hu X, Kong W and Zhang HH: Effect of catch-up growth after food restriction on the entero-insular axis in rats. Nutr Metab(Lond) 7: 45, 2010.
22. Bedossa P, Poitou C, Veyrie N, Bouillot JL, Basdevant A, Paradis V, Tordjman J and Clement K: Histopathological algorithm and scoring system for evaluation of liver lesions in morbidly obese patients. Hepatology 56: 1751-1759, 2012.
23. Kleiner DE, Brunt EM, Van Natta M, Behling C, Contos MJ, Cummings OW, Ferrell LD, Liu YC, Torbenson MS, Unalp-Arida A, *et al*: Design and validation of a histological scoring system for nonalcoholic fatty liver disease. Hepatology 41: 1313-1321, 2005.
24. Livak KJ and Schmittgen TD: Analysis of relative gene expression data using real-time quantitative PCR and the 2(-Delta Delta C(T)) method. Methods 25: 402-408, 2001.
25. Pierantonelli I and Svegliati-Baroni G: Nonalcoholic fatty liver disease: Basic pathogenetic mechanisms in the progression from NAFLD to NASH. Transplantation 103: e1-e13, 2019.
26. Li P, Li Y, Zhu L, Yang Z, He J, Wang L, Shang Q, Pan H, Wang H, Ma X, *et al*: Targeting secreted cytokine BMP9 gates the attenuation of hepatic fibrosis. Biochim Biophys Acta Mol Basis Dis 1864: 709-720, 2018.
27. Flores-Costa R, Alcaraz-Quiles J, Titos E, López-Vicario C, Casulleras M, Duran-Güell M, Rius B, Diaz A, Hall K, Shea C, *et al*: The soluble guanylate cyclase stimulator IW-1973 prevents inflammation and fibrosis in experimental non-alcoholic steatohepatitis. Br J Pharmacol 175: 953-967, 2018.
28. Roderfeld M: Matrix metalloproteinase functions in hepatic injury and fibrosis. Matrix Biol 68-69: 452-462, 2018.
29. Berres ML, Nellen A and Wasmuth HE: Chemokines as immune mediators of liver diseases related to the metabolic syndrome. Dig Dis 28: 192-196, 2010.
30. Deshmane SL, Kremlev S, Amini S and Sawaya BE: Monocyte chemoattractant protein-1 (MCP-1): An overview. J Interferon Cytokine Res 29: 313-326, 2009.
31. Upton PD, Davies RJ, Trembath RC and Morrell NW: Bone morphogenetic protein (BMP) and activin type II receptors balance BMP9 signals mediated by activin receptor-like kinase-1 in human pulmonary artery endothelial cells. J Biol Chem 284: 15794-15804, 2009.
32. Appleby SL, Mitrofan CG, Crosby A, Hoenderdos K, Lodge K, Upton PD, Yates CM, Nash GB, Chilvers ER and Morrell NW: Bone morphogenetic protein 9 enhances lipopolysaccharide-induced leukocyte recruitment to the vascular endothelium. J Immunol 197: 3302-3314, 2016.
33. Young K, Conley B, Romero D, Tweedie E, O'Neill C, Pinz I, Brogan L, Lindner V, Liaw L and Vary CP: BMP9 regulates endoglin-dependent chemokine responses in endothelial cells. Blood 120: 4263-4273, 2012.
34. Rocher C and Singla DK: SMAD-PI3K-Akt-mTOR pathway mediates BMP-7 polarization of monocytes into M2 macrophages. PloS One 8: e84009, 2013.
35. Martínez VG, Rubio C, Martinez-Fernandez M, Segovia C, López-Calderón F, Garín MI, Teijeira A, Munera-Maravilla E, Varas A, Sacedón R, *et al*: BMP4 induces M2 macrophage polarization and favors tumor progression in Bladder cancer. Clin Cancer Res 23: 7388-7399, 2017.
36. Moore LB, Sawyer AJ, Charokopos A, Skokos EA and Kyriakides TR: Loss of monocyte chemoattractant protein-1 alters macrophage polarization and reduces NFkappaB activation in the foreign body response. Acta Biomater 11: 37-47, 2015.